

## CONTRAST ENHANCEMENT FOR MULTI-MODALITY IMAGE FUSION IN SPATIAL DOMAIN

<sup>1</sup>NADA JASIM HABEEB, <sup>2</sup>ALI AL-TAEI, <sup>3</sup>MOHAMMED FADHIL-IBRAHIM

<sup>1</sup>Middle Technical University, Technical College of Management, Baghdad, Iraq

<sup>2</sup>Reconstruction and Projects Office, Ministry of Higher Education and Scientific Research, Baghdad, Iraq

<sup>3</sup>Middle Technical University, Technical College of Management, Baghdad, Iraq

### ABSTRACT

In some scenes that cover a large area, some of the cameras capture images that may be affected by weather conditions or illumination changes, this causes the exposure of these images to a lack of focus, blur, or/and noise. Multi-model image fusion is a significant technique in computer vision and image processing to solve these problems. In this paper, a multi-model image fusion is proposed and presented in three case studies. Each case has a different scheme and all cases have the same goal. The goal of the proposed algorithm is to enhance the source images in spatial domain before fusion process leading to increase the quality of fused image. The techniques, which are used in the proposed method, are Principle Component Analysis, Histogram Equalization; sharpen filter, and Weighted Averaging fusion. Comparison analysis is achieved using some focus measurements to test the performance of the proposed algorithm in the three cases comparing with the baseline fusion techniques. The experimental results showed that the proposed method obtains better performance in preserving gradation contrast and enhancing fused image quality.

**Keywords:** *Multi-model image fusion, Histogram Equalization, sharpen filter, Principle Component Analysis, Weighted Averaging fusion, focus metrics*

### 1. INTRODUCTION

Image fusion is used to improve the quality of image by the combining multiple registered images. Image fusion depends on two factors: (1) image registration and (2) fusing relevant features from the registered images. Image registration is the process which aligns two or more image data sets that are captured in the same scene by different sensors or at different viewpoints [1]. The goal of image fusion is to enhance human visual system, robotic visual system, computer vision, and image processing. Multi-focus images and infrared-visible images are examples of image modalities that are used for better situation awareness and visibility enhancement.

The Multi-modality image fusion combines the information of registered multi-modality images of same scene. Many applications use multi-modality image fusion such as military applications, robotics, weather forecasting, and so on. In general image fusion is achieved in three levels: pixel-level, feature-level, and decision-level. The pixel-level fusion is the most common level. It is the lower level fusion in which the pixels of the

source images are fused directly. The benefit of this type of fusion is that the fused image contains high accuracy information and more detail information [2]. Compared with the other two levels, the pixel level fusion is computationally efficient, easy to implement and widely used. It can be performed in spatial domain, transform domain, or in both domains. Comprehensive survey of this fusion level can be found in [3].

Many image fusion techniques were proposed at spatial domain such as Weighted Averaging (WA) based image fusion, principle component analysis based image fusion, intensity-hue-saturation based image fusion, etc... These methods are easy implemented and offer better results. The disadvantages of these methods are: leading to reduction of sharpness, unclear edges, and contrast decrease. Transform-domain based methods use a transform tool to decompose multiple images into coefficients. Then the coefficients are fused using fusion rules. Finally, inverse transform is applied to obtain a final fused image [4]. Discrete Wavelet Transform, Dual-Tree Complex Wavelet Transform, Curvelet Transform, etc. were implemented to solve the problems of

spatial domain based image fusion. However, some problems of poor image quality still exist [5]. Recent years, many image fusion techniques were proposed. To obtain high-resolution multispectral (MS) image, the panchromatic and MS images are fused in the spatial domain, in [6], the authors proposed a fusion method using non-subsample Shear-let transform (NSST) containing the following steps: First, color space transform using the intensity–hue–saturation transformation. Second, multi-resolution analysis based methods are used to solve the insufficiency of spatial de-tail in resampled images. Third, fusion rules are applied using a guided filter to obtain low-frequency coefficient and using Sum-Modified-Laplacian filter to obtain high-frequency coefficient. Finally, inverse NSST and IHS transform were performed to obtain the final fused image.

Image fusion for medical imaging is an important tool to enhance visual perception. The authors in [7] proposed an image fusion technique to localize anomalies in bone and vessel images. First, Karhunen-Loeve transformations and Rippled transforms are used. Second, the anisotropic diffusion filtering is used to remove noise and artefacts of the result. Finally, the fusion process is applied using Laplacian pyramid decomposition to fuse the obtaining mask and DSA images. In [8], the author presented multi-modality images fusion which exploits the advantages of the transform and spatial domain techniques. First, the source images are decomposed using wavelet transform. Second, the transformed coefficients are fused based on the fusion rules. Third, the initial fused image is acquired using the inverse wavelet transform. Finally, to increase image reliability, the edges of the focused part of input images are extracted and replaced with edges in the initial fused image. The work in [9], the authors provided a fusion method for multi-spectral images by combining Block-DCT and PCA to provide quality enhancement with preserving the spatial resolution.

In [10] the author presented a multi-focus image fusion using combination of lifting DWT and PCA. In this paper. Lifting Wavelet Transform decomposed the input images into four sub-bands. Secondly, the of source images Principal Component Analysis is applied on each sub-band. The new sub-band is generated by selected maximum eigenvector. The fused image is created by performing the Inverse Lifting Wavelet Transform.

The work in [11] the author proposed a multi-sensor image fusion technique for hyperspectral images containing two stages of

guided filter in PCA domain. First, down-sampling is performed on the Higher Resolution of Colour image to the same spatial resolution of low resolution of hyperspectral image, and guided filter is applied to transfer the image details of the down-sampled colour image to the original low resolution of hyperspectral image in the PCA domain. Second, upsampling is applied on the hyperspectral image resulted from the previous stage by using original high resolution of colour image and finally, the guided filter is applied in the PCA domain. The work in [12] proposed a feature level fusion for ear recognition system using PCA. The proposed algorithm divided the input image into blocks, and then PCA is applied on each block. The fusion process is achieved at feature and classification level.

For fusion of two types of medical images, CT-MRI and MRI images, the authors in [13] proposed Image fusion method to fuse the two images using DWT and PCA. DWT decomposes source images into multiscale inputs and then the principal components are evaluated for the coefficients. Weighted average is used as fusion rule to fuse the relevant decomposed elements. In [14], the author developed hybrid Multi-sensor image fusion technique using directional Discrete Cosine Transform and Principal Component Analysis. The input images are segmented into blocks. The fusion process is applied on the corresponding blocks. To achieve the fusion process on the corresponding coefficients between two images, three different fusion rules are used: averaging, choosing maximum energy and choosing maximum absolute value. Principle component analysis based fusion is used to obtain the final fused image.

In this paper, we focus on the problem of multi-model image fusion using pixel wise averaging technique. The result of this method is blurred image with low contrast. In order to obtain better gradation contrast and good fused image observation a fusion method based on Principle Component Analysis, Histogram Equalization, sharpen filter, and weighted average is proposed for multi-model images such as visible and infrared images. The idea of this method is to enhance the contrast of the source images before performing of the fusion process. The proposed multi-model image fusion is fast and simple method and improves the sharpness and contrast of the fused image. The benefits of the result of the proposed method are providing better visual perception and it more convenient for better understanding and

analysis. Furthermore, it produces dimensional reduction for source images.

The paper is organized as follows: section 2 presents the theory which is related the topics of this research. In section 3 the schemes of the proposed method are presented in three case studies. Section 4 describes the experimental results. Finally, conclusions are presented in section 5.

## 2. THEORY

### 2.1 Principle component Analysis

The basic idea of Principle Component Analysis (PCA) was to reduce the dimensions of the data set consisting of a large number of variables while maintaining the variance in the data set. PCA transforms the correlated variables into linearly uncorrelated variables, which preserves most of the variation in all the original variables. In other words, a thick line on the left in Fig. 1 indicates to the largest variance, which represents the first component (PC1) and the new x-axis. Then, PCA algorithm searches the new y-axis (PC2) which is orthogonal to the x-axis. The two new dimensions hold the variation in the image data [15, 12].

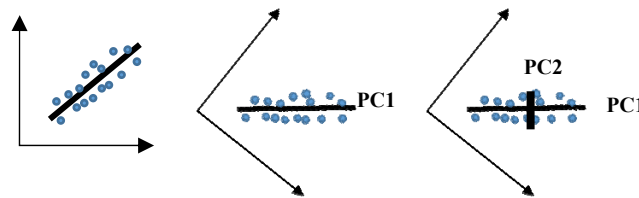


Fig. 1. Searching Principle Components in 2D-data.

### 2.2 Histogram Equalization

Histogram Equalization is the most common techniques used for enhancement image contrast in a spatial domain by adjusting image intensities. The contrast is defined as the difference in intensity between two objects in an image. If the contrast is too low, it is impossible to distinguish between two objects and they are seen as a single object. The idea of HE is to spread out the displayed brightness levels in the peak areas and compressing other parts of the histogram [16]. This method is useful when an image has background and foreground are bright at the same time, or are dark at the same time. If there are grey values that

are different from each other in the image, then this method is not produce good results.

### 2.3 Weighted Averaging Fusion

Pixel weighted averaging based fusion is a simple technique and can be used to remove noise from the source images [17, 24]. The disadvantage of this technique is stressing the salient features of fused image, this will produce a low contrast images. Weighted Averaging of k images is used to solve this problem by using Eq. (1).

$$fusedimage(m, n) = \frac{\sum_{k=1}^N w_k I_k(m, n)}{\sum_{k=1}^N w_k} \quad (1)$$

where  $W_k$  is pre-selected weights.

### 2.4 Sharpen Filter

The main objective of sharpening the image is to increase the clarity of the fine details of the image such as the edges of the objects that suffer from the blur and lack of clarity. Sharpening process is considered as a pre-processing step to increase contrast between bright and dark areas for highlighting the edge features of the image [18].

Laplacian operator is the most popular function for sharpening image. It is isotropic derivative operator, which can be defend by the following equations (Eq. (2) and Eq. (3)):

$$\nabla^2 f(i, j) = f(i + 1, j) + f(i - 1, j) + f(i, j + 1) + f(i, j - 1) - 4f(i, j) \quad (2)$$

$$\nabla^2 f(i, j) = f(i + 1, j - 1) + f(i + 1, j) + f(i + 1, j + 1) + f(i - 1, j - 1) + f(i - 1, j) + f(i - 1, j + 1) + f(i, j - 1) + f(i, j + 1) - 8f(i, j) \quad (3)$$

From the above equations, the Laplacian can be represented as matrices, Fig.2 shows different Laplacian masks.

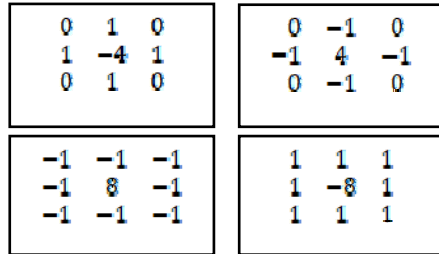


Fig. 2. Laplacian masks

### 2.5 Evaluation Metrics

A good result of fusion algorithm should have the following features:

- i. The result of fusion algorithm should contain the important information from the input images.
- ii. The fused image does not contain any visual artifacts and it should clear for the human observation system, computer vision, and image processing.
- iii. The result of fusion algorithm should be empty from noise and blurriness.

Estimating image focus is an essential problem in computer vision and image processing because a dimension of image is lost during the projection from the three dimension image in real world to a two-dimension image in digital imaging [19]. In order to evaluate the results of proposed methods, some no-reference focus measure operators were selected. When the reference of the fused image is available, some full-reference quality metrics also were selected. Table 1 (Appendix section) illustrates no-reference focus metrics.

### 2.6 Proposed Image Fusion

In this work, different visible-infrared images that were captured on different scenes are used to test the proposed fusion method. The proposed method is represented in three case studies, which are presented to show which one

gives better results. The proposed fusion schemes are shown in Fig. 3, Fig.4, and Fig.5.

The proposed algorithm in case study (1), Fig.3 can be illustrated as follows:

Firstly, PCA algorithm is applied on both source images (Visible image (Vis) and Infrared image (IR)); PCA plays an important role in dimensional reduction.

Secondly, Histogram Equalization (HE) is applied to the result of PCA for Vis image and Sharpen Filter (SF) is applied to the result of PCA for IR image. The purpose of using HE is to enhance Vis image, which has less quality, and the purpose of using SF is to increase the focus of IR image because in the nature infrared image suffers from blurriness.

Finally, the new image is obtained by using pixel wise Weighted Averaging fusion, which fuses enhanced Vis image and focused IR image.

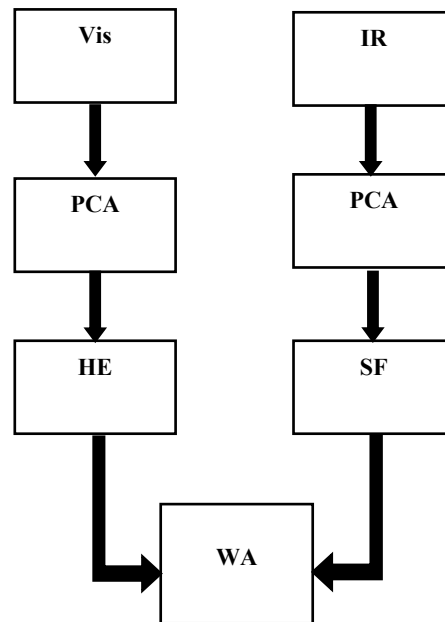


Fig. 3. The scheme of case study (1)

The proposed algorithm in case study (2), Fig.4, can be illustrated as follows: first, HE is applied on Vis image and SF is applied on IR image, then dimension reduction is performed by using PCA for both enhanced images. Finally, the

new image is obtained by using Weighted Averaging fusion, which fuses enhanced Vis image and focused IR image.

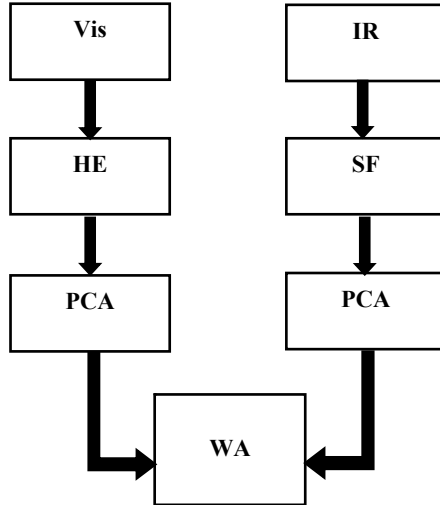


Fig. 4. The scheme of case study (2)

The proposed algorithm in case study (3), Fig.5, can be illustrated as follows: first, dimension reduction is performed by using PCA for both Vis and IR images, then enhancement of both images is achieved by using HE. Finally, the new image is obtained by using Weighted Averaging fusion to obtain a new image by fusing enhanced Vis and IR images.

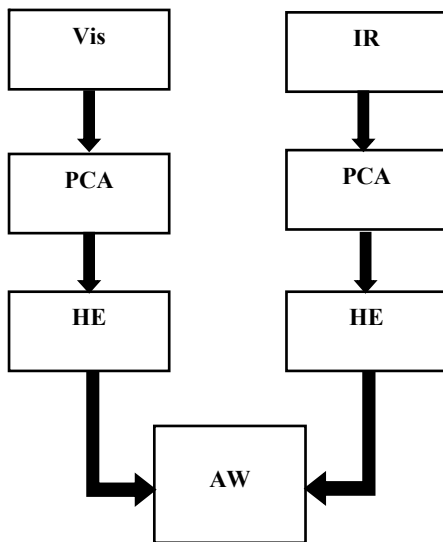


Fig. 5. The scheme of case study (3)

### 3. EXPERIMENTAL RESULTS

Three types of multi-model images, which are City, Street, and trees scenes (see Fig. 7), were used for testing the performance of the traditional and proposed image fusion methods. The traditional fusion methods that are used in this work are PCA based image fusion and image averaging based fusion.

In case (1) and case (2), the fusion algorithm used sharpening Laplacian filter in one time and a proposed sharpen filter in another time to enhance the focus of infrared image. The fusion algorithm, which used the proposed sharpening mask, gives better results than using Laplacian mask. The proposed sharpen mask is illustrated in Fig. 6. An example in Fig. 8 shows the visual results of the proposed method in the case study (1). Table 1 – Table 10 show the numerical results of the comparison of the existing and the proposed methods on multi-model image based on the selected focus operators.

|    |    |    |
|----|----|----|
| 0  | -1 | -1 |
| -1 | 9  | -1 |
| -1 | -2 | -1 |

Fig. 6. The proposed sharpen mask

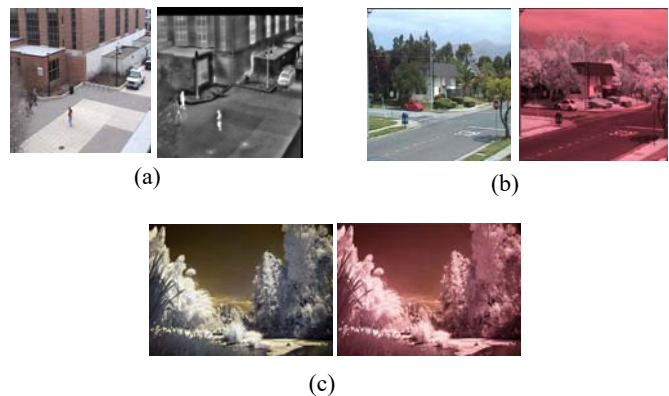


Fig. 7. The source images

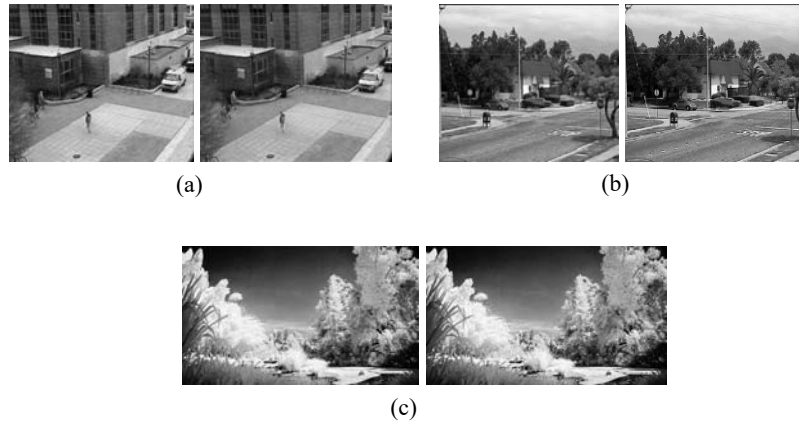


Fig. 8. The visual results of the proposed fusion in case study (1)

Table 2. Case (1): Comparison results of the existing and the proposed methods on multi-model image - city scene.

| Metrics\Fusion | Traditional Method-Averaging | PCA based fusion  | Proposed Method with Laplacian filter | Proposed Method with proposed filter |
|----------------|------------------------------|-------------------|---------------------------------------|--------------------------------------|
| ACM            | 3.2986e+04                   | <b>3.7552e+04</b> | 2.9442e+04                            | <b>3.0668e+04</b>                    |
| CONT           | 36.5613                      | 51.6139           | 50.0281                               | <b>57.7596</b>                       |
| GDER           | 174.4109                     | <b>357.8977</b>   | 271.7055                              | <b>326.8693</b>                      |
| GLVA           | 43.5358                      | <b>61.5151</b>    | 55.6946                               | <b>60.8419</b>                       |
| GRAE           | 52.8654                      | 67.1034           | 72.3240                               | <b>81.9375</b>                       |
| HISE           | 7.2963                       | 7.7013            | 7.6674                                | <b>7.7922</b>                        |

Table 3. Case (1): Comparison results of the existing and the proposed methods on multi-model image - street scene.

| Metrics\Fusion | Traditional Method-Averaging | PCA based fusion | Proposed Method with Laplacian filter | Proposed Method with proposed filter |
|----------------|------------------------------|------------------|---------------------------------------|--------------------------------------|
| ACM            | <b>3.3289e+04</b>            | 3.1668e+04       | 3.1412e+04                            | <b>3.1690e+04</b>                    |
| CONT           | 45.6816                      | 40.4842          | 61.3373                               | <b>66.7657</b>                       |
| GDER           | 374.6229                     | 307.4507         | 531.6433                              | <b>545.4374</b>                      |
| GLVA           | 55.8392                      | 50.0217          | 67.2259                               | <b>68.1476</b>                       |
| GRAE           | 58.1348                      | 54.5973          | 74.4859                               | <b>81.3452</b>                       |
| HISE           | 7.5375                       | 7.4376           | 7.9122                                | <b>7.9299</b>                        |

**Table 4.** Case (1): Comparison results of the existing and the proposed methods on multi-model image - trees scene.

| Metrics\Fusion | Traditional Method-Averaging | PCA based fusion | Proposed Method with Laplacian filter | Proposed Method with proposed filter |
|----------------|------------------------------|------------------|---------------------------------------|--------------------------------------|
| ACM            | 2.6633e+04                   | 2.6070e+04       | 2.6472e+04                            | <b>3.1872e+04</b>                    |
| CONT           | 65.1876                      | 68.5774          | <b>107.0621</b>                       | <b>94.4047</b>                       |
| GDER           | 309.0124                     | 326.7494         | 300.9039                              | <b>380.2210</b>                      |
| GLVA           | 59.1195                      | 60.9893          | 62.4440                               | <b>72.4164</b>                       |
| GRAE           | 80.0923                      | 81.5718          | <b>98.2378</b>                        | <b>95.9093</b>                       |
| HISE           | 7.6014                       | 7.6397           | 7.6480                                | <b>7.9789</b>                        |

**Table 5.** Case (2): Comparison results of the existing and the proposed methods on multi-model image - city scene.

| Metrics\Fusion | Traditional Method-Averaging | PCA based fusion  | Proposed Method with Laplacian filter | Proposed Method with proposed filter |
|----------------|------------------------------|-------------------|---------------------------------------|--------------------------------------|
| ACM            | 3.2986e+04                   | <b>3.7552e+04</b> | 3.0102e+04                            | <b>3.0701e+04</b>                    |
| CONT           | 36.5613                      | 51.6139           | 56.9112                               | <b>61.2816</b>                       |
| GDER           | 174.4109                     | <b>357.8977</b>   | 294.1329                              | <b>326.6098</b>                      |
| GLVA           | 43.5358                      | <b>61.5151</b>    | 58.3653                               | <b>61.1399</b>                       |
| GRAE           | 52.8654                      | 67.1034           | 82.3599                               | <b>87.9875</b>                       |
| HISE           | 7.2963                       | 7.7013            | 7.7347                                | <b>7.8011</b>                        |

**Table 6.** Case (2): Comparison results of the existing and the proposed methods on multi-model image – street scene.

| Metrics\Fusion | Traditional Method-Averaging | PCA based fusion | Proposed Method with Laplacian filter | Proposed Method with proposed filter |
|----------------|------------------------------|------------------|---------------------------------------|--------------------------------------|
| ACM            | 3.3289e+04                   | 3.1668e+04       | 2.4118e+04                            | <b>3.1657e+04</b>                    |
| CONT           | 45.6816                      | 40.4842          | <b>148.6867</b>                       | <b>65.0061</b>                       |
| GDER           | 374.6229                     | 307.4507         | 309.2047                              | <b>543.8330</b>                      |
| GLVA           | 55.8392                      | 50.0217          | 60.3118                               | <b>68.0710</b>                       |
| GRAE           | 58.1348                      | 54.5973          | <b>114.2752</b>                       | <b>78.1101</b>                       |
| HISE           | 7.5375                       | 7.4376           | 7.6835                                | <b>7.9289</b>                        |

| Metrics\Fusion | Traditional Method-Averaging | PCA based fusion | Proposed Method with Laplacian filter | Proposed Method with proposed filter |
|----------------|------------------------------|------------------|---------------------------------------|--------------------------------------|
| ACM            | 2.6633e+04                   | 2.6070e+04       | <b>3.2081e+04</b>                     | <b>3.1850e+04</b>                    |
| CONT           | 65.1876                      | 68.5774          | 84.6064                               | <b>90.5253</b>                       |
| GDER           | 309.0124                     | 326.7494         | <b>394.9926</b>                       | <b>382.2450</b>                      |
| GLVA           | 59.1195                      | 60.9893          | <b>72.7979</b>                        | <b>72.3497</b>                       |
| GRAE           | 80.0923                      | 81.5718          | 89.3464                               | <b>93.5957</b>                       |
| HISE           | 7.6014                       | 7.6397           | <b>7.9850</b>                         | <b>7.9837</b>                        |

Table 8. Case (3): Comparison results of the existing and the proposed methods on multi-model image –city scene.

| Metrics\Fusion | Traditional Method-Averaging | PCA based fusion  | Proposed Method   |
|----------------|------------------------------|-------------------|-------------------|
| ACM            | 3.2986e+04                   | <b>3.7552e+04</b> | 3.2413e+04        |
| CONT           | 36.5613                      | <b>51.6139</b>    | 48.6591           |
| GDER           | 174.4109                     | 357.8977          | <b>1.0800e+03</b> |
| GLVA           | 43.5358                      | 61.5151           | <b>66.3982</b>    |
| GRAE           | 52.8654                      | 67.1034           | <b>68.6524</b>    |
| HISE           | 7.2963                       | 7.7013            | <b>7.8166</b>     |

Table 9. Case (3): Comparison results of the existing and the proposed methods on multi-model image – street scene.

| Metrics\Fusion | Traditional Method-Averaging | PCA based fusion | Proposed Method   |
|----------------|------------------------------|------------------|-------------------|
| ACM            | 3.3289e+04                   | 3.1668e+04       | <b>3.5299e+04</b> |
| CONT           | 45.6816                      | 40.4842          | <b>67.5241</b>    |
| GDER           | 374.6229                     | 307.4507         | <b>727.4722</b>   |
| GLVA           | 55.8392                      | 50.0217          | <b>79.0589</b>    |
| GRAE           | 58.1348                      | 54.5973          | <b>76.2235</b>    |
| HISE           | 7.5375                       | 7.4376           | <b>7.7476</b>     |



**Table 10.** Case (3): Comparison results of the existing and the proposed methods on multi-model image – tree scene.

| Metrics\Fusion | Traditional Method-Averaging | Traditional Method-PCA | Proposed Method   |
|----------------|------------------------------|------------------------|-------------------|
| ACM            | 2.6633e+04                   | 2.6070e+04             | <b>3.5212e+04</b> |
| CONT           | 65.1876                      | 68.5774                | <b>86.6914</b>    |
| GDER           | 309.0124                     | 326.7494               | <b>455.8900</b>   |
| GLVA           | 59.1195                      | 60.9893                | <b>78.4419</b>    |
| GRAE           | 80.0923                      | 81.5718                | <b>85.9118</b>    |
| HISE           | 7.6014                       | 7.6397                 | <b>7.8082</b>     |

For numerical comparative, some focus metrics (see Table (1)) were used. Table (2), Table (3), and Table (4) show the comparison analysis between the traditional and the proposed methods for case study (1)

In Table (2), the proposed fusion that uses the proposed sharpen mask gives good quality results compared with the traditional Weighted Averaging fusion and the proposed method using Laplacian filter. Some metric values in PCA based fusion are higher than others in ACM, GDER, and GLVA. In Table (3), the proposed fusion using the proposed sharpen mask produces higher values compared with the others. Except ACM value for traditional Weighted Averaging fusion is highest value. In Table (4), Image contrast (CONT) and Gradient energy (GRAE) for proposed method that uses Laplacian filter indicated good results compared with the others.

Table (5), Table (6), and Table (7) show the numerical analysis between the traditional methods and the proposed methods for case study (2). In Table (5) Proposed Method with proposed sharpening mask gives good quality results, except ACM, GDER, and GLVA for PCA based fusion which produce higher values compared with others.

In table (6), higher quality values are produced by the proposed fusion with using proposed mask against the other fusion methods.

Proposed method with Laplacian filter gives best results in CONT and GRAE metrics and PCA

based image fusion also gives good quality value in ACM metric. In Table (7), the proposed fusion method using the proposed mask produces better results. The proposed method using Laplacian mask gives good results in GDER, GDER, and HISE metrics. Table (8), Table (9), and Table (10) show the numerical analysis between the traditional method and the proposed methods for case study (3). In this case, the proposed fusion algorithm produced better results compared with other algorithms, except in Table (8), PCA based fusion produces better results in ACM and CONT metrics.

#### 4. CONCLUSION

In this paper, the proposed multi-model image fusion is presented in three case studies. The techniques that are used in the proposed algorithms are Histogram Equalization, sharpen filters, and Weighted Averaging fusion which is represented as a fusion rule. Histogram Equalization is used to enhance an image that has less contrast quality, while sharpen filters are used to increase the focus for blurry image. The contribution of this research is to enhance the contrast of source images before performing the fusion process. This gives better fusion results. The proposed algorithms were tested on three multi-model image datasets. Comparisons with other fusion approaches were performed using some selected focus metrics. The experimental results of the proposed method showed better results against some baseline approaches. The variation in results during the three cases depends on the features (color, size, texture, and so on) of the source image.

**REFERENCES:**

- [1] James, Alex Pappachen, and Belur V. Dasarathy. "Medical image fusion: A survey of the state of the art." *Information Fusion* 19 (2014): 4-19.
- [2] Li, Weisheng, Jia Zhao, and Bin Xiao. "Multimodal medical image fusion by cloud model theory." *Signal, Image and Video Processing* 12.3 (2018): 437-444.
- [3] Li, S., Kang, X., Fang, L., Hu, J., & Yin, H. (2017). Pixel-level image fusion: A survey of the state of the art. *Information Fusion*, 33, 100-112.
- [4] Nandal, Amita, and Hamurabi Gamboa Rosales. "Enhanced image fusion using directional contrast rules in fuzzy transform domain." *SpringerPlus* 5.1 (2016): 1846.
- [5] Wu, Zhiliang, Yongdong Huang, and Kang Zhang. "Remote Sensing Image Fusion Method Based on PCA and Curvelet Transform." *Journal of the Indian Society of Remote Sensing* (2018): 1-9.
- [6] Wan, Weiguo, Yong Yang, and Hyo Jong Lee. "Practical remote sensing image fusion method based on guided filter and improved SML in the NSST domain." *Signal, Image and Video Processing* (2018): 1-8.
- [7] Dogra, Ayush, Bhawna Goyal, and Sunil Agrawal. "Osseous and digital subtraction angiography image fusion via various enhancement schemes and Laplacian pyramid transformations." *Future Generation Computer Systems* (2018).
- [8] Paramanandham, Nirmala, and Kishore Rajendiran. "Multi sensor image fusion for surveillance applications using hybrid image fusion algorithm." *Multimedia Tools and Applications* (2017): 1-32.
- [9] Saboori, Arash, and Javad Birjandtalab. "Remote sensing image data fusion using spatial PCA and average block-DCT." *Signal Processing and Communication Systems (ICSPCS)*, 2016 10th International Conference on. IEEE, 2016.
- [10] Aymaz, Samet, and Cemal Köse. "Multi-focus image fusion using Stationary Wavelet Transform (SWT) with Principal Component Analysis (PCA)." *Electrical and Electronics Engineering (ELECO)*, 2017 10th International Conference on. IEEE, 2017.
- [11] Liao, W., Huang, X., Van Coillie, F., Thoonen, G., Pižurica, A., Scheunders, P., & Philips, W. (2016, June). Two-stage fusion of thermal hyperspectral and visible RGB image by PCA and Guided filter. In *Hyperspectral Image and Signal Processing: Evolution in Remote Sensing (WHISPERS)*, 2015 7th Workshop on (pp. 1-4). IEEE.
- [12] Tharwat, A., Ibrahim, A., Hassanien, A. E., & Schaefer, G. (2015, June). Ear recognition using block-based principal component analysis and decision fusion. In *International Conference on Pattern Recognition and Machine Intelligence* (pp. 246-254). Springer, Cham.
- [13] Vijayarajan, R., and S. Muttan. "Discrete wavelet transform based principal component averaging fusion for medical images." *AEU-International Journal of Electronics and Communications* 69.6 (2015): 896-902.
- [14] Naidu, V. P. S. "Hybrid DDCT-PCA based multi sensor image fusion." *Journal of Optics* 43.1 (2014): 48-61.
- [15] Silirtola, Harri, Tanja Säily, and Terttu Nevalainen. "Interactive Principal Component Analysis." *Information Visualisation (IV)*, 2017 21st International Conference. IEEE, 2017.
- [16] Russ, John C. *The image processing handbook*. CRC press, 2016.
- [17] Mönks, Uwe, et al. "Information fusion of conflicting input data." *Sensors* 16.11 (2016): 1798.
- [18] Jeevakala, S. "Sharpening enhancement technique for MR images to enhance the segmentation." *Biomedical Signal Processing and Control* 41 (2018): 21-30.
- [19] Pertuz, Said, Domenech Puig, and Miguel Angel Garcia. "Analysis of focus measure operators for shape-from-focus." *Pattern Recognition* 46.5 (2013): 1415-1432.
- [20] Nanda, Harsh, and Ross Cutler. "Practical calibrations for a real-time digital omnidirectional camera." *CVPR Technical Sketch* 20 (2001).
- [21] H. Xie, W. Rong, L. Sun, Wavelet-based focus measure and 3-d surface reconstruction method for microscopy images, in: *Proceedings of the IEEE/RSJ International Conference on Intelligent Robots and Systems*, 2006, pp. 229-234.
- [22] Sun, Yu, Stefan Duthaler, and Bradley J. Nelson. "Autofocusing in computer microscopy: selecting the optimal focus algorithm." *Microscopy research and technique* 65.3 (2004): 139-149.
- [23] Huang, Wei, and Zhongliang Jing. "Evaluation of focus measures in multi-focus image fusion." *Pattern Recognition Letters* 28.4 (2007): 493-500.
- [24] Habeeb, Nada, Saad Hasson, and Phil Picton. "Multi-Sensor Fusion based on DWT, Fuzzy Histogram Equalization for Video Sequence." *analysis* 13.14: 22. 2018.

APPENDIX

Table 1 illustrates the focus operators that are used for testing the performance the algorithms in this work.

Table 1. No Reference Focus Metrics

| Metric name                   | format                                                                                                                                                                                                                                                                                                                                                          | Description |
|-------------------------------|-----------------------------------------------------------------------------------------------------------------------------------------------------------------------------------------------------------------------------------------------------------------------------------------------------------------------------------------------------------------|-------------|
| absolute central moment (ACM) | <p>ACM Based on statistical measures and the image histogram</p> $ACM = \sum_{k=1}^L  k - \mu  P_k$ <p>Where <math>\mu</math> is the mean intensity value of the image histogram, <math>L</math> is the gray levels, and <math>P_k</math> is the frequency of k-th gray level.</p>                                                                              | [19]        |
| Image contrast (CONT)         | $C(x,y) = \sum_{i=x-1}^{x+1} \sum_{j=y-1}^{y+1}  f(x,y) - f(i,j) $ <p>where <math>C(x,y)</math> is the image contrast for pixel <math>f(x,y)</math></p>                                                                                                                                                                                                         | [20]        |
| Gaussian derivative (GDER)    | <p>a focus measure based on the first order Gaussian derivative</p> $FM = \sum_{(x,y)} (f * G_x)^2 + (f * G_y)^2$ <p>Where <math>G_x</math> and <math>G_y</math> are the x and y partial derivatives of the Gaussian function <math>G(x,y,\sigma)</math>, respectively</p> $G(x,y,\sigma) = \frac{1}{2\pi\sigma^2} \exp\left(-\frac{x^2+y^2}{2\sigma^2}\right)$ | [19]        |
| Gradient energy (GRAE)        | $FM_{x,y} = \sum_{(i,j) \in \Omega(x,y)} (f_x(i,j)^2 + f_y(i,j)^2)$                                                                                                                                                                                                                                                                                             | [21]        |
| Histogram entropy (HISTE)     | <p>The histogram entropy operator is defined as</p> $FM = - \sum_{k=1}^L P_k \log(P_k)$ <p>Where <math>P_k</math> is the relative frequency of the k-th grey-level.</p>                                                                                                                                                                                         | [22]        |